Journal of Crystal Growth 584 (2022) 126557

Contents lists available at ScienceDirect

Journal of Crystal Growth

journal homepage: www.elsevier.com/locate/jcrysgro

Hydrodynamically driven facet kinetics in crystal growth

Mihaela Stefan-Kharicha [a], Abdellah Kharicha [a,*], Kader Zaidat [b], Georg Reiss [c], Werner Eßl [c], Frank Goodwin [d], Menghuai Wu [a], Andreas Ludwig [a], Claudia Mugrauer [b]

[a] Montanuniversitaet Leoben, Leoben, Austria
[b] Univ. Grenoble Alpes, CNRS, Grenoble INP, SIMaP, F-38000 Grenoble, France
[c] Material Center Leoben, Leoben, Austria
[d] International Zinc Association, United States

ARTICLE INFO

Communicated by Srinivasan Manickam

Keywords:
A1. Computer simulation
A1. Fluid flows
A1. Growth models
A1. Convection
A2. Single crystal growth
A2. Growth from melt

ABSTRACT

In this paper we show that the presence of liquid flow around a crystal growing from melt can induce dissymmetry in growth similar to that described by anisotropic interfacial kinetic coefficients. A front tracking interface model based on a cellular automaton approach was applied to the growth of a Fe_2Al_5 crystal (also known as top dross particle) in a saturated Zn melt at constant temperature. The growth rate was found to be influenced by the intensity of the melt flow and by the direction of the flow with respect to the crystal orientation. The magnitude and the direction of flow modify the diffusion boundary layer, changing the conditions (temperature and concentration) at the facet interface, therefore the mass transfer. We have shown that despite the isotropy of interfacial kinetics, hydrodynamics was able to introduce an anisotropy in the crystal growth similar to the natural anisotropy in interfacial kinetics of the facets. The facets grow rate was found to be strongly dependant on the Reynolds number as well as on the orientation of the crystalline orientation with respect to the flow direction.

1. Introduction

Anisotropy plays an important role in the development of faceted crystal growth. Thermodynamics, interface kinetics and surfaces energy can be very different from one facet to the other, resulting in faster growth by some facets and slower growth by others. Faster growing facets can disappear leaving a corner or edges as boundary between the slower adjacent faces.

Many examples of faceted crystals exhibiting anisotropic growth can be found in nature or industrial production. Si crystals are ubiquitous in the electronic industry and therefore the growth of Si crystals is well understood. Fujiwara et al. [1] directly observed the growth behaviour of Si in an undercooled region. They determined experimentally the critical undercooling for faceted dendrite growth to be 10 K. The parallel twins associated with faceted dendrite growth were formed between grain boundaries and not at grain boundaries during melt growth. The parallel-twin formation was explained in terms of a model of twin formation on the {1 1 1} facet plane at the growth interface.

In-situ growth of benzophenone from melt was performed under various cooling rates and temperature gradients [2]. The growth rate of all the faces increased with the cooling rate of the melt. Steady state growth was observed for small temperature gradients while unstable growth was observed at steeper gradients (>0.4 C mm). Moreover, it was found that the growth rate varied with different faces. A high growth rate was observed for (0 0 1) face and a low growth rate was observed for (0 1 1) face. The growth anisotropy was attributed to variations in the intermolecular binding energies of the respective growth faces.

LaFeAsO large crystals obtained by Kappenberger et al. [3] show pronounced facets and a large growth rate along the c axis. This was obtained by a new strategy using solid state single crystal growth, where the growth was diffusion controlled.

In the aforementioned examples, asymmetry in the crystal growth was related to anisotropic thermodynamics and interfacial kinetics. Sizaret et al. [4–5] have theoretically shown that flow hydrodynamic can also induce an asymmetry. They investigated the influence of the flow on the growth of a triangular shaped crystal in 2D (calcite). The growth of the facet and its final shape, was found to be influenced by the angle between the flow and the facet. Larger angles slowed the growth rate of the facet. The growth rate decreased downstream resulting in a

* Corresponding author.
E-mail address: abdellah.kharicha@unileoben.ac.at (A. Kharicha).

https://doi.org/10.1016/j.jcrysgro.2022.126557
Received 9 October 2021; Received in revised form 5 January 2022; Accepted 24 January 2022
Available online 31 January 2022

Table 1
Physical properties of liquid Zinc and simulation parameters.

Properties/characteristics	Values
ρ_l (density)	6600 kg/m^3
c_p (heat capacity)	512 J/kg•K
λ (thermal conductivity)	60 W/m^2•K
μ_l (viscosity)	0.0034 kg/m•s
D_l (diffusivity)	1.75•10^{-9} m^2/s (450 °C)
K_2 (interfacial kinetic coefficient)	1.14•10^{-8} s^{-1}
T (Gibbs-Thomson coefficient)	5.5•10^{-7} m•K
C_0 (initial liquid concentration in Fe)	0.02 wt%
C_S (solid concentration in the crystal)	0.7 wt%

more elongated crystal. The analytical results are in good agreement to the observed natural calcite crystals. Beside the natural growth anisotropy, the hydrodynamic of the flow around the growing crystal is able to induce a growth anisotropy. In our previous paper [6] it was shown numerically that without flow all facets of a Fe_2Al_5 crystal grow at the same rate. The growth rate was controlled by the combined action of the interface kinetics and the isotropic diffusion around the crystals. In presence of a flow, the diffusion layer loses its isotropy. The upstream facets were found to grow faster than the downwind ones.

In the current paper, this topic is further investigated to explore the importance of the crystal orientation with respect to the flow direction. To illustrate only the influence of the flow direction and magnitude, the crystal is assumed to have the same interface kinetics and surface energy for all crystallographic directions. The model is applied to the 2D growth of an isothermal hexagonal Fe_2Al_5 crystal in a supersaturated liquid zinc alloy, as in the previous paper [6].

2. Growth model and simulation settings

The growth model was presented in a previous paper [6]. In the following a short summary is given. The model considered a cellular automaton (CA) with a front tracking method at the solid/liquid interface. The envelope of the crystal is tracked in a Lagrangian way with "numerical tracers". With this method, all directions of crystal growth can be correctly modelled, for any Eulerian mesh orientation.Interface kinetics, together with solute transport by diffusion and convection are considered. The model differentiates the normal growth from the lateral growth at the kinks. In the numerical simulations the lateral growth is modeled by introducing a numerical kink kinetic. Due to its fast kinetics, interface concentration of a numerical kink is assumed to be very close to the thermodynamic equilibrium. At the facets, a kinetic supersaturation is added in the calculation of the interface concentration. Thus, mass transfer at kinks is much faster than that at facets. This allows the development of relatively flat facets. The flow and solute transport are modelled with a volume averaging approach [7]. The model solves the conservation equations of mass, momentum, and species for a binary mixture, leading to a fluid–solid system [6]. In the flow simulation a penalty factor is used in order to account for the presence of growing crystal, which is considered as an obstacle for the flow.

The quadratic kinetic growth law is given in previous paper [6]. The physical properties of the liquid Zinc, the interfacial kinetic coefficient K_2, the Gibbs-Thomson coefficient, as well as the initial liquid and solid concentrations can be found in Table 1. The interfacial kinetic coefficient K_2, has the same value for all facets, as well as the Gibbs-Thomson

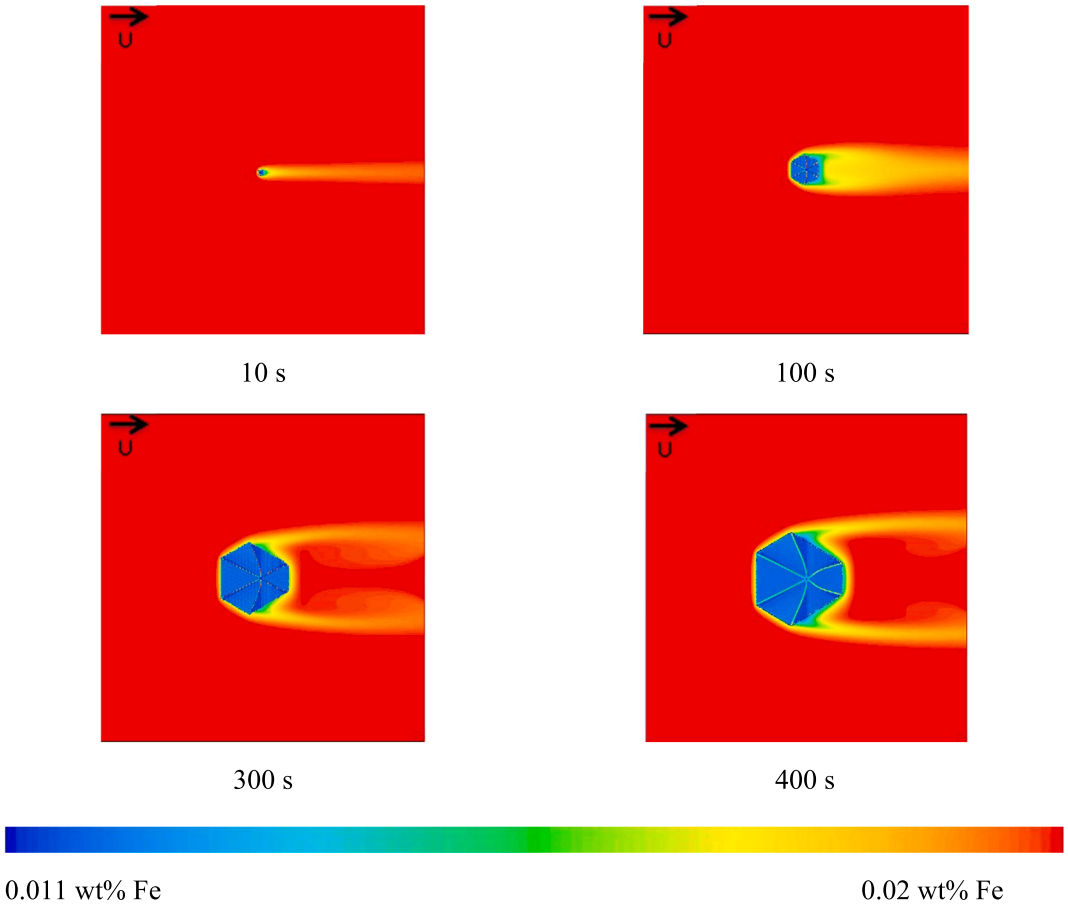

Fig. 1. Crystal (dark blue) evolution under 0.36 m/s melt flow and the corresponding Fe concentration field in the liquid around the crystal. Colours inside the crystal indicate the trajectory of the tracers used for the interface tracing. (For interpretation of the references to colour in this figure legend, the reader is referred to the web version of this article.)

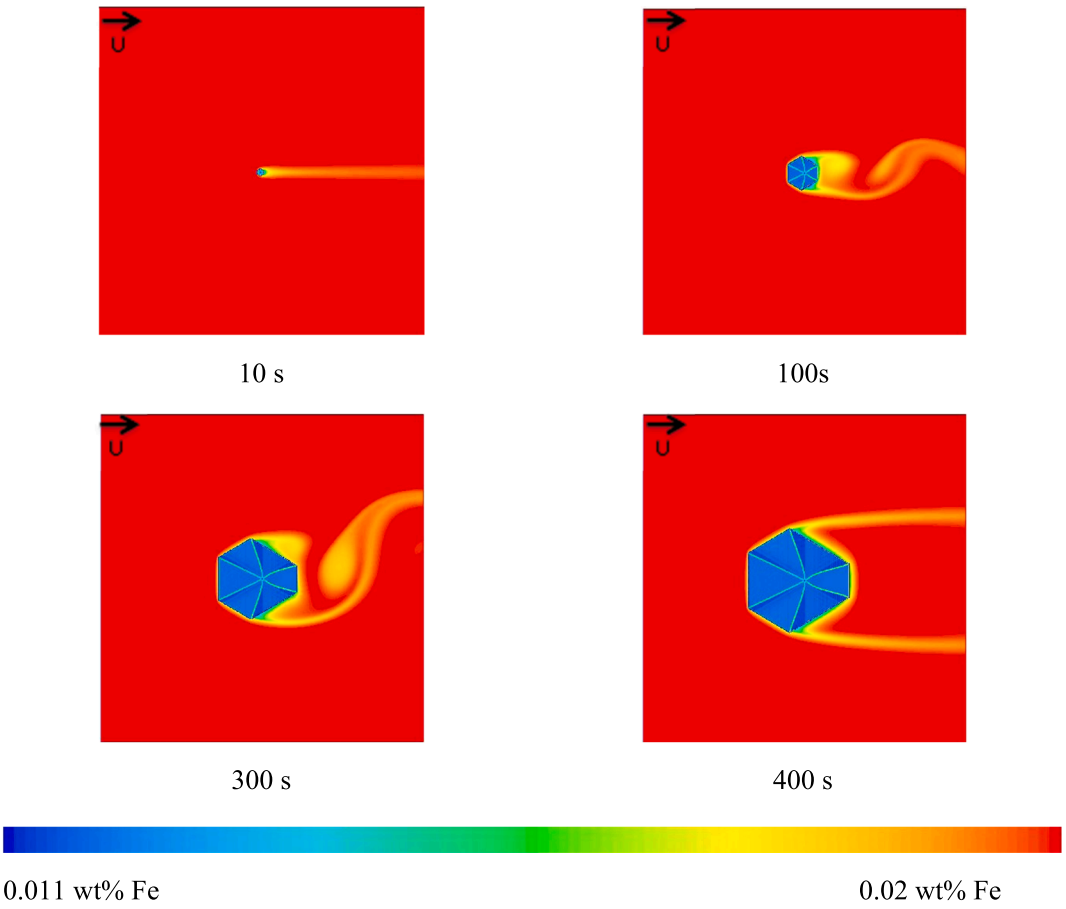

Fig. 2. Crystal (dark blue) evolution under 0.72 m/s melt flow and the corresponding Fe concentration field in the liquid around the crystal. Colours inside the crystal indicate the trajectory of the tracers used for the interface tracing. (For interpretation of the references to colour in this figure legend, the reader is referred to the web version of this article.)

coefficient. The 2D simulations start with a perfect hexagonal crystal of 1 μm size, in a square domain of 600*600 μm^2. The left boundary is an inlet which provides a constant velocity U and iron concentration C_0. The up and down boundary are slipping walls and pressure outlet is applied at the right boundary. The initial crystal is placed exactly in the middle of the domain. The crystal orientation geometry corresponds to a 30° shifting compared to the configuration studied in [6] where the flow direction faced a corner of the crystal.

Several situations are simulated with relative melt velocities between 0.36 m/s and 1.44 m/s. These situations reproduce the velocity conditions of Fe_2Al_5 crystal growth at the surface of a roll submerged in a zinc bath during the industrial Hot-Dip Galvanizing process.

3. Results

The flow velocity and concentration C_0 are imposed at the left inlet boundary. The crystal's facet at the left-hand side of the pictures, where the flow comes perpendicular to the facet, is called *front facet*, opposite the facet at the right-hand side of the pictures, called *back facet*. Additionally, we define the top and the bottom facets, where the flow is parallel to the facets. Figs. 1–3 present the results of the faceted crystal growth at different melt flow velocities. The iron concentration is shown only in the liquid surrounding the crystal, inside the crystal the concentration is constant (see Table 1).

For all cases presented in Figs. 1–3 it can be observed that the diffusion boundary layer is not similar for the different crystal facets. At the front facets the boundary diffusion layer is much thinner than at the other facets. Furthermore, with the increase of the melt flow velocity it can be observed that the solute diffusion boundary layer becomes even thinner.

Already at around 100 s (second pictures in Figs. 1–3) it can be observed that the crystal starts losing its symmetry; the initial centre point is "moved to the right" of the developed crystal. The upstream part of the crystal has grown faster as its downwind part. Asymmetry is also observed in the fact that some tracers of the corner's positions (colour inside the solid crystal) are not straight lines, but rather bended. This phenomenon is particularly strong in the beginning of the growth ($t < 300$ s). Since a corner marks the boundary between two facets, the bend of the line formed by the corner tracers indicates that a facet is faster than its adjacent one. For larger time $t > 300$ s, i.e. for larger crystals, the corner positions seem straighter than at the beginning of the growth.

For all cases (0.36 m/s, 0.72 m/s and 1.44 m/s melt flow), unstable flow was observed, starting with approximately 149 s, 58 s and respectively 22 s. It results from the occurrence of the so called von Kármán vortices (evidence of von Kármán vortices is given in second and third pictures in Figs. 2 and 3). H. Karampour et al. [8] showed that for a flow around a hexagon, the von Kármán vortices appear at a critical Reynolds (*Re*) number between 54 and 55. The dimensionless *Re* number was calculated as follows: $Re = \frac{\rho_l U L_2}{\mu_l}$, where L_2 is the length of the crystal perpendicular to the flow direction and U is the melt flow velocity. In the present study the corresponding critical *Re* number value,

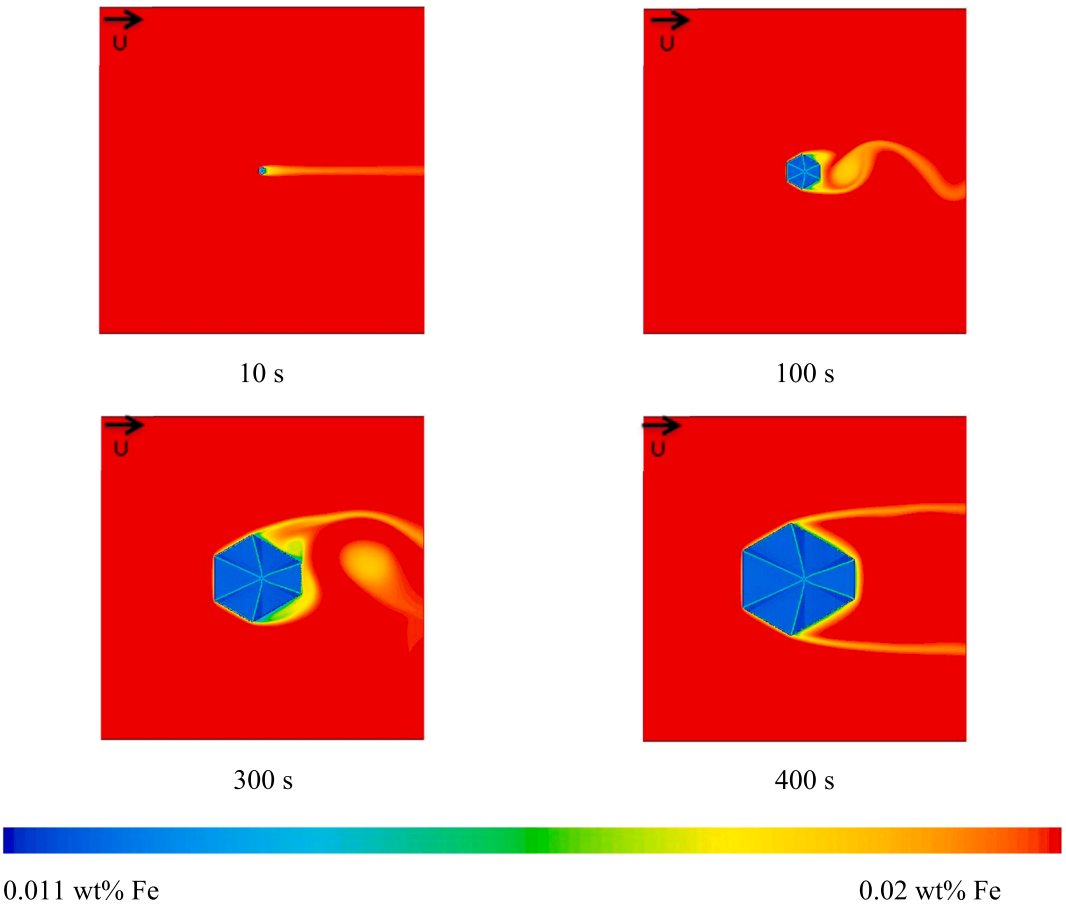

Fig. 3. Crystal (dark blue) evolution under 1.44 m/s melt flow and the corresponding Fe concentration field in the liquid around the crystal. Colours inside the crystal indicate the trajectory of the tracers used for the interface tracing. (For interpretation of the references to colour in this figure legend, the reader is referred to the web version of this article.)

for the above presented simulations, turned out to be approximately 53.

In Fig. 4 the upstream facets (marked by r_{front}) are growing faster than the downstream facets (marked by r_{back}). This results from the fact that due to hydrodynamics, the diffusion boundary layer is thinner at the front facets than at the back ones, consequently the growth at the front facets is faster. Therefore, the mass transfer is faster at the front than at the back of the crystal and the crystal shape becomes more elongated to the back. Moreover, the growth is faster with the increase of the flow intensity. The same remarks can be drawn as for the length of the front and back facets (Fig. 5); for all flow velocity cases the growth of the length of the facets (front and back) follows a linear relation. The length of the front facet of the crystal increases always faster than the length of the back facet of the crystal, for all melt velocities. The facet length's growth rate increases with the flow velocity increase.

This can be correlated to the boundary diffusion layer, which is much thinner for the upstream facets than for the downwind ones.

Knowing these results, it is possible to analyse the evolution of the ratio between the front and the back crystal radius (Fig. 6).

The ratio between the front radius and the back radius doesn't follow the same trend for all flow velocities (Fig. 6). For the smaller flow velocity 0.36 m/s the ratio is increasing very fast until a quasi-constant value ~1.4, which means there was a 40% more growth at the front facet than at the back facet. At the beginning the crystal grows faster at its upstream side than at its downstream side, therefore the ratio is >1 and increases in time. Later at $t > 200$ s, a quasi-plateau is reached, the crystal grows with the same growth rate on the upstream and at the downstream sides. This plateau is corresponding to the occurrence of von Kármán vortices, which bring rich solute liquid towards the back of the crystal. These vortices increase the mass transfer at the back facets, limiting the front to back radius ratio. The growth at the upstream part is in a kind of equilibrium with the growth at the downstream part of the crystal.

For the two others larger velocities (0.72 m/s and 1.44 m/s) the radius ratio shows more unstable behaviour (Fig. 6). The crystal growth seems to have three growth phases in these cases of larger flow velocity (0.72 m/s and 1.44 m/s): (i) the upstream part grows faster than the downstream part (radius ratio increases until approximately 150 s in Fig. 6); (ii) then the downstream part grows faster than the upstream part (radius ratio decreases between 150 s and 200 s in Fig. 6); (iii) finally, the upstream part grows faster than the downstream part (the radius ratio increases after 200 s in Fig. 6).

This effect is related to the chaotic behaviour of the von Kármán vortices at Reynolds numbers higher than *Rec* ~ 150-(transition vortex sheet) which becomes less regular than for small Reynolds numbers. The Reynolds number can be estimated by considering the size ($\mathbf{r}_{front} + \mathbf{r}_{back}$) as the typical crystal size. Using values given in Fig. 4, *Rec* is reached at $t \sim 200 - 250$ s for 1.44 m/s and $t \sim 350 - 400$ s for 0.72 m/s. After these times the radius ratio further increases, this means that the mass transfer progressively decreases at the crystal's back in favour of the crystal's front. If the evolution of the ratio between the front radius and back radius of the crystal is different, the final value after 800 s of calculation, is similar for the three cases.

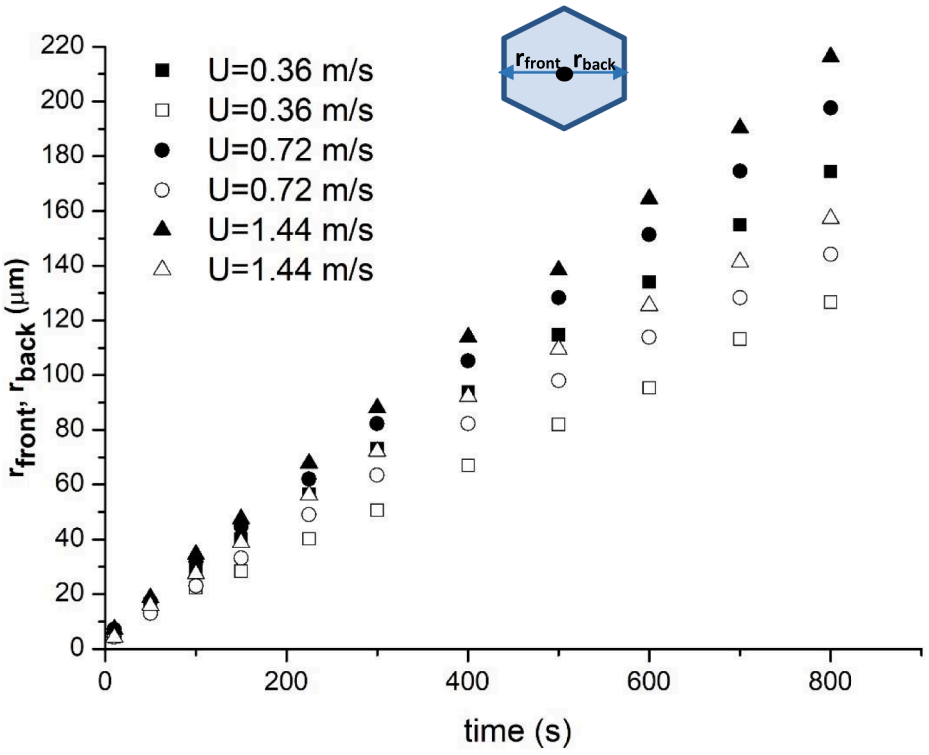

Fig. 4. Evolution of the radius size in time (filled forms represent the front radius of the crystal and empty forms represent the back radius of the crystal), for different flow velocities.

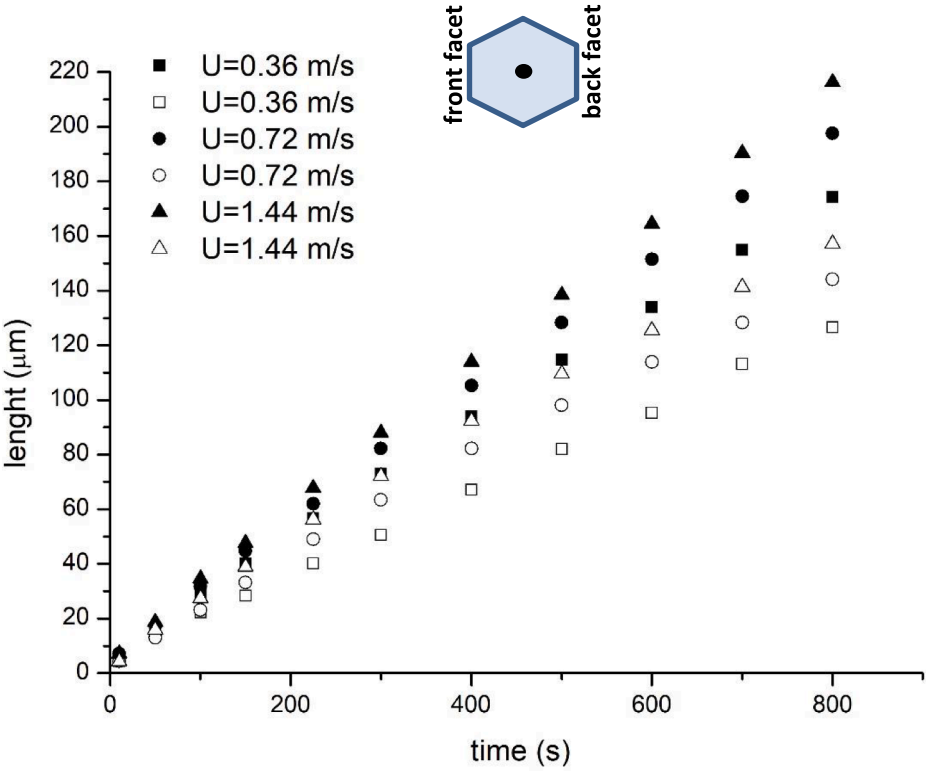

Fig. 5. Evolution of the crystal's facets length in time (filled forms represent the length of the front facet's crystal and empty forms represent the length of the back facet's crystal) for different flow velocities.

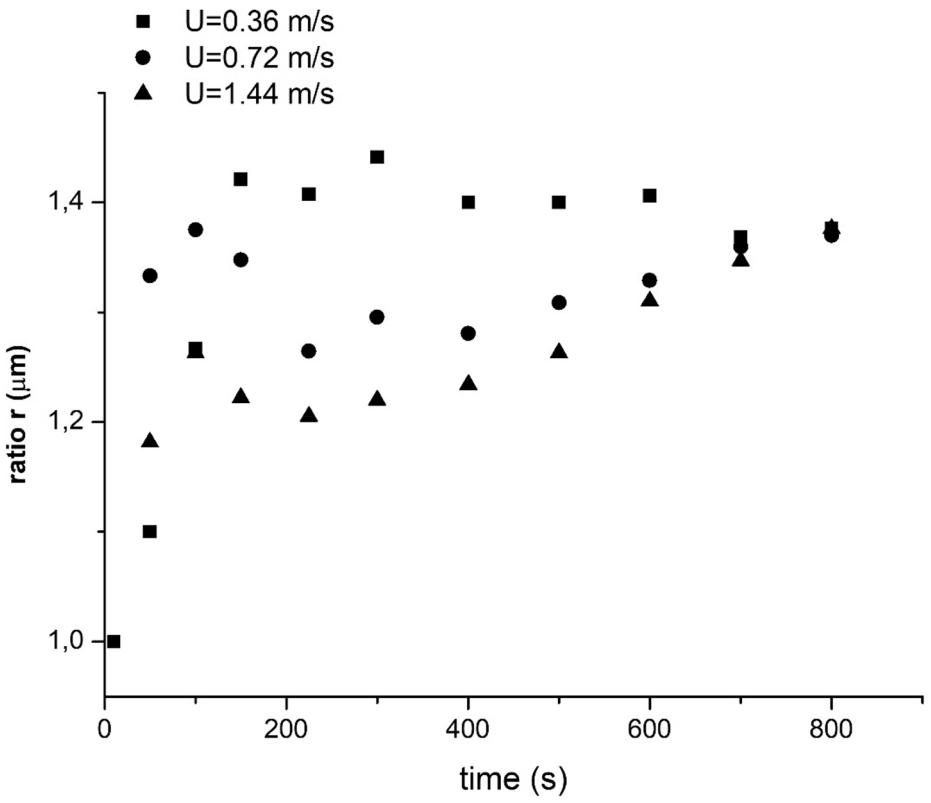

Fig. 6. Evolution in time of the ratio between the front radius (see Fig. 4) to the back radius, for different flow velocities.

This is also the reason why the crystal shape at 400 s (Figs. 1–3) seems less asymmetric for the higher melt velocities (0.72 m/s and 1.44 m/s) than at lower flow velocity (0.36 m/s). At 400 s the front to back radius ratio has a much larger value for the 0.36 m/s than for the higher melt velocities (0.72 m/s and 1.44 m/s).

The width (L1) and height (L2) of the crystal for the two orientations of the flow: towards the corner [6] and towards the facet (current work) of the crystal were measured and compared (Fig. 7). The width of the crystal (L1) is growing faster for the case of the flow coming towards the corner than for the case of the flow coming towards the facet (Fig. 7a). This can be explained by the so-called corner effect, next to the corners local peaks in mass transfer can be observed [9]. The near corner mass transfer is Reynolds number dependent, secondary flow vortices turning around the corner increases the mass transfer. In our case when the flow reaches the corner of the crystal the mass transfer is highly enhanced at the two adjacent facets, therefore the width of the crystals is growing faster in this case. For the height of the crystal (L2) at lower melt velocity (0.36 m/s) there is no difference between the two crystal orientations (Fig. 7b). For the larger flow velocities (0.72 m/s and 1.44 m/s) the height of the crystal is growing faster for the case when flow comes towards the facet than for the case when flow comes towards the corner. This situation is the opposite that was observed for the width of the crystal and it is due to the orientation of the crystal with respect to the flow. The mass transfer at the up and down corners (corner effect) encountered in the facets oriented crystal case, is stronger than that at the top and bottom facets, met in the corner crystal orientation. Therefore, the height will growth naturally faster in the configuration with flow towards facets.

4. Conclusions

The cellular automaton model employed here was able to simulate the growth of faceted crystal. One single crystal was simulated using a quadratic kinetic growth law, in the presence of melt flow impinging perpendicular to the crystal facet. Different melt flow velocities were simulated. In all the cases the model was able to keep the facets flat as observed in experiments.

This crystal was found to grow faster as melt flow velocity increased. The diffusion boundary layer is reduced in presence of melt flow, therefore the mass transfer and consequently growth rate is faster in presence of flow.

An important fact was observed for all cases: an asymmetry of the crystal facets growth was introduced by the melt flow magnitude and direction. The hydrodynamic influence on faceted crystal growth was clearly shown from evidence presented in this paper. The presence of the flow made the upstream part of the crystal (front facet) to grow faster than the downstream part (back facet), resulting in an elongated crystal. The flow hydrodynamics is able to induce a similar effect to that caused by natural anisotropy in a faceted crystal. Furthermore, the influence of the flow on the growth of the faceted crystal was found to be complex. A stronger effect was observed on the crystal width, when the flow is coming towards the corner, but a less strong effect on the height of the crystal. The oposite was observed when the flow impinges perpendicularly on the facet. The effect of the flow orientation with respect to the crystal was put in evidence. It could be expected that some facets disappear in time, but longer simulation time and larger domain are necessary in order to observe it in simulation.

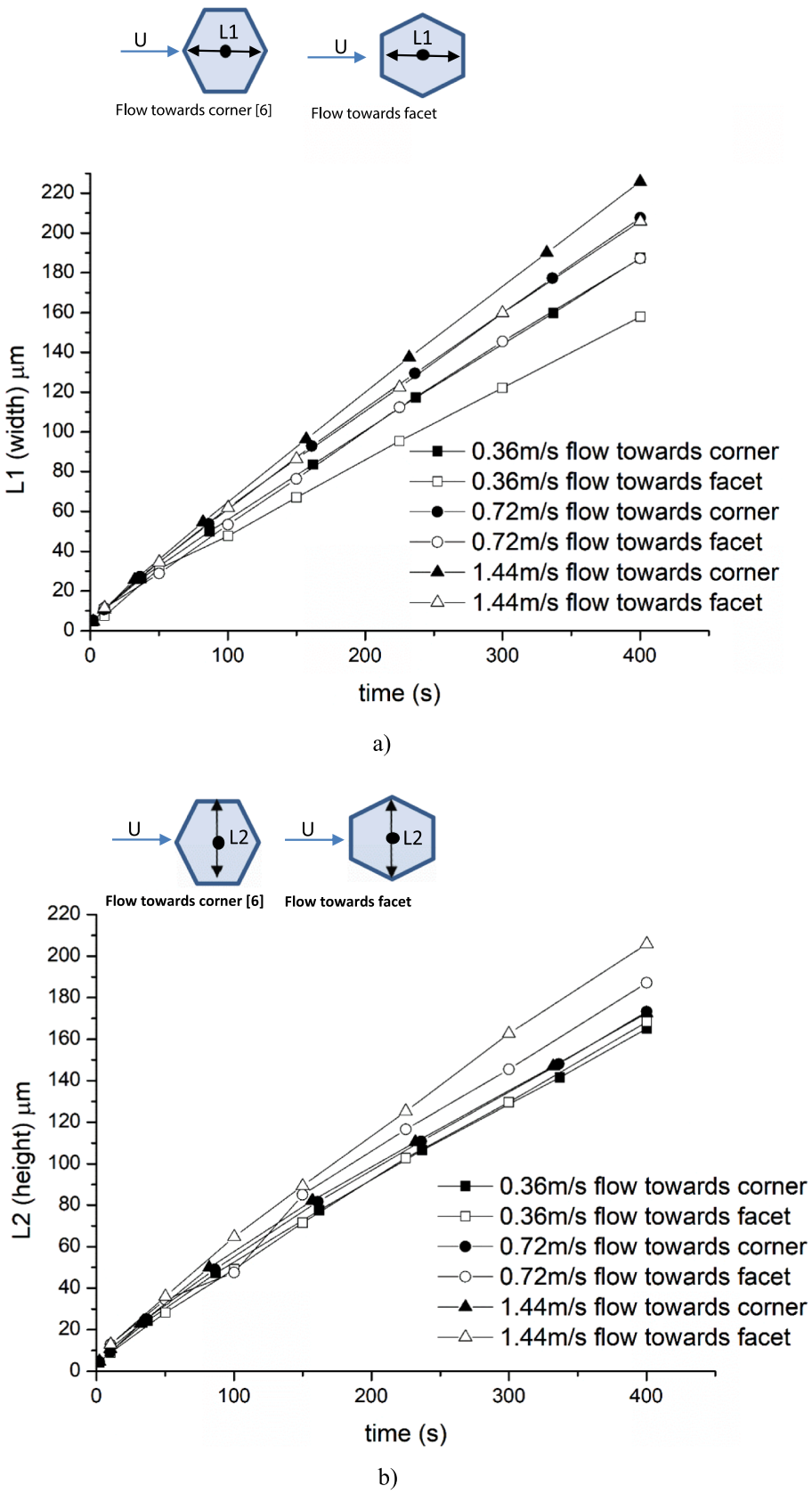

Fig. 7. Evolution of: (a) width (L1) and (b) height (L2) of the crystal for the two crystal orientations, flow towards the corner and flow towards the facet.

CRediT authorship contribution statement

Mihaela Stefan-Kharicha: Writing – original draft, Visualization, Investigation. **Abdellah Kharicha:** Conceptualization, Supervision, Writing – review & editing. **Kader Zaidat:** Conceptualization. **Georg Reiss:** Writing – review & editing. **Werner Eßl:** Writing – review & editing. **Frank Goodwin:** Writing – review & editing. **Menghuai Wu:** Conceptualization. **Andreas Ludwig:** Conceptualization. **Claudia Mugrauer:** Writing – review & editing.

Declaration of Competing Interest

The authors declare that they have no known competing financial interests or personal relationships that could have appeared to influence the work reported in this paper.

Acknowledgement

The authors gratefully acknowledge the financial support under the scope of the COMET program within the K2 Center "Integrated Computational Material, Process and Product Engineering (IC-MPPE)" (Project No 859480). This program is supported by the Austrian Federal Ministries for Climate Action, Environment, Energy, Mobility, Innovation and Technology (BMK) and for Digital and Economic Affairs (BMDW), represented by the Austrian research funding association (FFG), and the federal states of Styria, Upper Austria and Tyrol.

References

[1] K. Fujiwara, K. Maeda, N. Usami, G. Sazaki, Y. Nose, A. Nomura, T. Shishido, K. Nakajima, Acta Mater. 56 (2008) 2663–2668.
[2] V. Natarajan, M. Arivanandhan, P. Anandan, K. Sankaranarayanan, G. Ravi, Y. Inatomi, Y. Hayakawa, Mater. Chem. Phys. 144 (2014) 402–408.
[3] R. Kappenberger, S. Aswartham, F. Scaravaggi, C.G.F. Blum, M.I. Sturza, A.U. B. Wolter, S. Wurmehl, B. Büchner, J. Cryst. Growth 483 (2018) 9–15.
[4] S. Sizaret, Y. Chen, L. Barbanson, B. Henry, P. Camps, E. Marcoux, Geophys. J. Int. 167 (2006) 605–612.
[5] S. Sizaret, I. Fedioun, L. Barbanson, Y. Chen, Geophys. J. Int. 167 (2006) 1027–1034.
[6] A. Kharicha, M. Stefan-Kharicha, K. Zaidat, G. Reiss, W. Eßl, F. Goodwin, M. Wu, A. Ludwig, C. Mugrauer, J. Crystal Growth 541 (2020), 125667.
[7] M. Wu, A. Ludwig, Metall. Mater. Trans. A 38 (2007) 1465.
[8] H. Karampour, Z. Wu, J. Lefebure, D.-S. Jeng, A. Etemad-Shahidi, B. Simpson, Proc. Instit. Civil Engineers – Eng. Comput. Mech. 171 (2018) 99–114.
[9] R.J. Goldstein, M.Y. Jabbari, J.P. Brekke, Wärme- und Stoffübertragung 27 (1992) 265–272.